

# Sprouty2 Association with B-Raf Is Regulated by Phosphorylation and Kinase Conformation

Suzanne C. Brady,<sup>1</sup> Mathew L. Coleman,<sup>2</sup> June Munro,<sup>1</sup> Stephan M. Feller,<sup>3</sup> Nicolas A. Morrice,<sup>4</sup> and Michael F. Olson<sup>1</sup>

<sup>1</sup>The Beatson Institute for Cancer Research, Glasgow, United Kingdom; <sup>2</sup>Henry Wellcome Building for Molecular Physiology and <sup>3</sup>Weatherall Institute of Molecular Medicine, John Radcliffe Hospital, University of Oxford, Oxford, United Kingdom; and <sup>4</sup>MRC Protein Phosphorylation Unit, University of Dundee, Dundee, United Kingdom

## Abstract

**Sprouty2 is a feedback regulator that controls the Ras/Raf/MEK/extracellular signal-regulated kinase mitogen-activated protein kinase (MAPK) pathway at multiple levels, one way being through direct interaction with Raf kinases. Consistent with a role as a tumor suppressor, Sprouty2 expression is often down-regulated in human cancers. However, Sprouty2 is up-regulated in some cancers, suggesting the existence of posttranscriptional mechanisms that permit evasion of Sprouty2-mediated antitumorigenic properties. We report that MAPK activation induces Sprouty2 phosphorylation on six serine residues, which reduced Sprouty2 association with wild-type B-Raf. Mutation of these six serines to nonphosphorylatable alanines increased the ability of Sprouty2 to inhibit growth factor-induced MAPK activation. Oncogenic B-Raf mutants such as B-Raf V600E did not associate with Sprouty2, but this resistance to Sprouty2 binding was not due to phosphorylation. Instead, the active kinase conformation induced by oncogenic mutation prevents Sprouty2 binding. These results reveal a dual mechanism that affects the Sprouty2/B-Raf interaction: Sprouty phosphorylation and B-Raf conformation.** [Cancer Res 2009;69(17):6773–81]

## Introduction

Sprouty was identified in a *Drosophila* screen for modifiers of airway branching induced by fibroblast growth factor (FGF) signaling (1). Four mammalian Sprouty orthologues (Sprouty1–4; Sprouty2 being the closest to *Drosophila* Sprouty; refs. 1–4) comprise a family of receptor tyrosine kinase feedback regulators that modulate the Ras/Raf/MEK/extracellular signal-regulated kinase (ERK) mitogen-activated protein kinase (MAPK) pathway (5). As a consequence, they regulate processes such as proliferation, survival, and motility in response to receptor tyrosine kinase activation and influence the development of many tissues (6).

Clinical and experimental evidence is consistent with Sprouty proteins being tumor suppressors. When overexpressed, Sprouty proteins suppressed proliferation of cultured tumor cells (7–9) and urethane-induced lung cancer in mice (10). Conversely, small interfering (siRNA)-mediated Sprouty2 knockdown induced melanocyte proliferation (11), whereas Sprouty2 deletion enhanced K-Ras-induced lung cancer in mice (12). If Sprouty genes were tumor

suppressors, expression would be expected to be repressed or lost in cancers, which has been observed in a variety of tumors (13–19). However, Sprouty levels are elevated in melanoma cells expressing oncogenic B-Raf (11, 20, 21) or N-Ras (20) and in gastrointestinal stromal tumors expressing activated c-Kit (22, 23), suggesting that there may be posttranscriptional mechanisms to evade its tumor-suppressive effects.

Sprouty proteins are composed of a variable NH<sub>2</sub> terminus and a highly conserved cysteine-rich COOH terminus (24), which regulate MAPK signaling at multiple levels depending on cell context and growth factor receptor activated. One way they inhibit MAPK activation is by directly interacting with and inhibiting activation of Raf kinases (11, 25–28). We reported previously that Sprouty2 did not associate with oncogenic B-Raf mutants, which allows for increased active ERK levels in melanoma cell lines expressing mutant B-Raf despite elevated Sprouty2 (11). In this study, we investigated the Sprouty2/B-Raf interaction and propose two factors that influence this association: Sprouty2 phosphorylation at specific sites and the B-Raf kinase domain conformation.

## Materials and Methods

**Plasmids and proteins.** pEF Myc-B-Raf constructs and pcDNA3 FLAG-Sprouty2 were described previously (11). pcDNA3 HA B-Raf was from W. Kolch (Beatson Institute). pEXV MEK:EE was from C.J. Marshall (Institute for Cancer Research). For site-directed mutagenesis, FLAG-Sprouty2 was subcloned into the Gateway vector system (Invitrogen) and point mutations were introduced using the QuikChange kit (Stratagene) according to the manufacturer's protocol.

Recombinant human wild-type and V600E glutathione-S-transferase (GST)-B-Raf catalytic domains were from Cell Signaling Technology or Millipore. FLAG-Sprouty2 was cloned into pGEX-4T3 (GE Healthcare) and expressed and purified using standard methods (29).

Alternatively, FLAG-Sprouty2 was subcloned into pGEX-6P3 (GE Healthcare) and expressed and purified as described above. Flag Sprouty2 was cleaved from GST by incubation with 80 units PreScission Protease (GE Healthcare) in cleavage buffer [50 mmol/L Tris (pH 7.5), 150 mmol/L NaCl, 1 mmol/L EDTA, 1 mmol/L DTT] for 4 h at 4°C.

*In vitro* transcribed and translated [<sup>35</sup>S]methionine-labeled HA B-Raf was generated from pcDNA3 HA B-Raf using the TNT T7 Quick Coupled Transcription Translation kit (Promega) according to the manufacturer's protocol.

**Cell culture and transfections.** HEK293 cells were cultured in DMEM supplemented with 10% (v/v) fetal bovine serum, 100 units/mL penicillin, and 100 µg/mL streptomycin (Invitrogen) at 37°C and 5% CO<sub>2</sub>. Cells were transfected with FuGENE6 (Roche) according to the manufacturer's protocol and harvested 24 h later. Amounts of wild-type and phosphorylation site mutant Sprouty2 plasmids transfected were adjusted to equilibrate protein levels.

Parental NIH3T3 cells were maintained in DMEM supplemented with 10% (v/v) donor calf serum (Invitrogen). Details of generation of Tet-Off Sprouty2 cell lines are in Supplementary Methods. Mouse embryo fibroblasts were maintained in DMEM with 10% (v/v) fetal bovine serum,

**Note:** Supplementary data for this article are available at Cancer Research Online (<http://cancerres.aacrjournals.org/>).

**Requests for reprints:** Michael F. Olson, The Beatson Institute for Cancer Research, Garscube Estate, Switchback Road, Glasgow G61 1BD, United Kingdom. Phone: 44-41-330-3654; Fax: 44-41-942-6521; E-mail: m.olson@beatson.gla.ac.uk.

©2009 American Association for Cancer Research.

doi:10.1158/0008-5472.CAN-08-4447

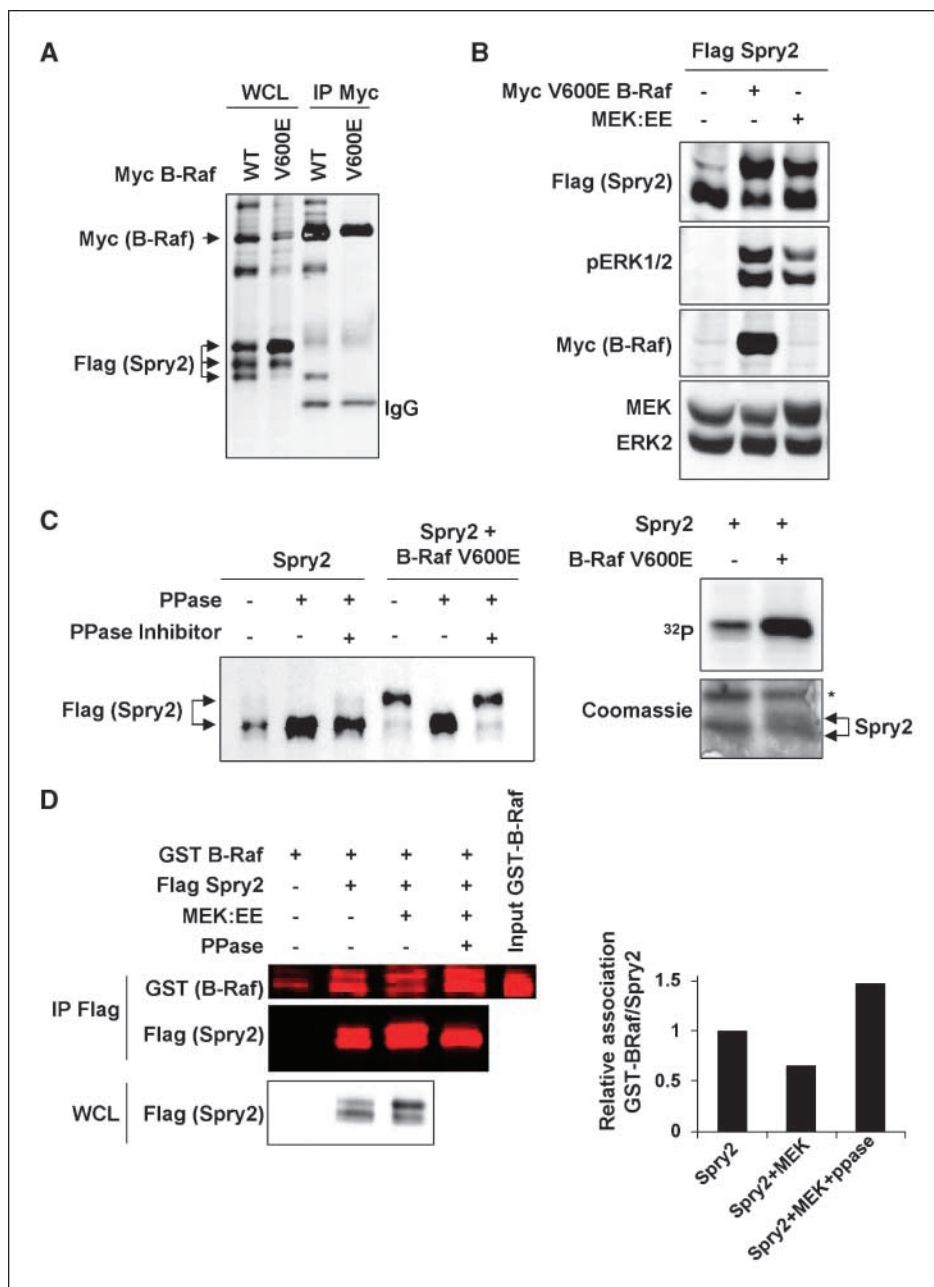


**Figure 1.** Sprouty2 phosphorylation regulates association with B-Raf. *A*, cells were transfected with FLAG-Sprouty2 (*Spry2*) and Myc-B-Raf wild-type (*WT*) or V600E. WCL and Myc immunoprecipitates (*IP Myc*) were Western blotted. *B*, Western blots of cells coexpressing FLAG-Sprouty2 and Myc-B-Raf V600E or MEK1:EE. *C*, *left*, FLAG-Sprouty2 transfected alone or with Myc-B-Raf V600E was immunoprecipitated and treated with calf intestinal phosphatase (*PPase*) and phosphatase inhibitor; *right*, metabolic  $^{32}\text{P}$  labeling of cells transfected with FLAG-Sprouty2 alone or with Myc-B-Raf V600E. Immunoprecipitated Sprouty2 was analyzed by autoradiography (*top*) and Coomassie staining (*bottom*). Asterisk, nonspecific protein. *D*, FLAG-Sprouty2 transfected alone or with MEK1:EE was immunoprecipitated. The sample coexpressed with MEK1:EE was divided into two and treated with or without phosphatase. Immunoprecipitated Sprouty2 was then incubated with GST-B-Raf catalytic domain and recovered by anti-FLAG immunoprecipitation. Anti-FLAG IP, WCL, and input GST-B-Raf were Western blotted for GST and/or FLAG.

100 units/mL penicillin, and 100  $\mu\text{g}/\text{mL}$  streptomycin at 37°C and 10%  $\text{CO}_2$ , and cell lysates were prepared as described in ref. 30.

**Cell extraction and immunoblotting.** Whole-cell lysates (WCL) were prepared and Western blotted as described previously (11). Primary antibodies used were as follows: murine anti-FLAG (Sigma-Aldrich), rabbit anti-Myc 9B11 (Cell Signaling Technology), murine anti-pERK1/2 (Cell Signaling Technology), rabbit anti-ERK1/2 (Millipore), rabbit anti-GST (Cell Signaling Technology), rabbit anti-Sprouty (Upstate Biotechnology), and rabbit anti-MEK (Cell Signaling Technology). Alexa Fluor 680 (Molecular Probes) or IRDye800 (Rockland)-conjugated secondary antibodies were detected by infrared imaging (Li-Cor Odyssey).

**Immunoprecipitations.** Myc-B-Raf complexes were immunoprecipitated from HEK293 WCL and analyzed for associated FLAG-Sprouty2 as described previously (11). Detailed methods can be found in Supplementary Methods.

**In vivo cell labeling.** HEK293 cells transiently expressing FLAG-Sprouty2 and Myc-B-Raf V600E were cultured overnight in phosphate-free

DMEM supplemented with 0.2 mCi/mL  $^{32}\text{P}$  (Amersham Biosciences). Cells were lysed in Tris lysis buffer [50 mmol/L Tris (pH 7.5), 150 mmol/L NaCl, 1% Triton, 1 mmol/L  $\text{Na}_3\text{VO}_4$ , 50 mmol/L NaF, 5 mmol/L  $\beta$ -glycerophosphate, 2 mmol/L EDTA, 1 mmol/L DTT, 1 mmol/L phenylmethylsulfonyl fluoride, and 1 $\times$  Complete protease inhibitor cocktail (Roche)]. FLAG-Sprouty2 was immunoprecipitated from WCL and analyzed by SDS-PAGE followed by Coomassie staining with Simply Blue SafeStain (Invitrogen) and autoradiography.

**Identification of Sprouty2 phosphorylation sites by mass spectrometry.** FLAG-Sprouty2 was immunoprecipitated from HEK293 cells, eluted with Laemmli buffer, separated by SDS-PAGE, and detected by staining with Brilliant Blue G Colloidal Coomassie (Sigma). Sprouty2 bands were excised, destained with successive ammonium bicarbonate and acetonitrile washes, and digested with trypsin as described previously (31). Extracted tryptic peptides were analyzed by liquid chromatography-mass



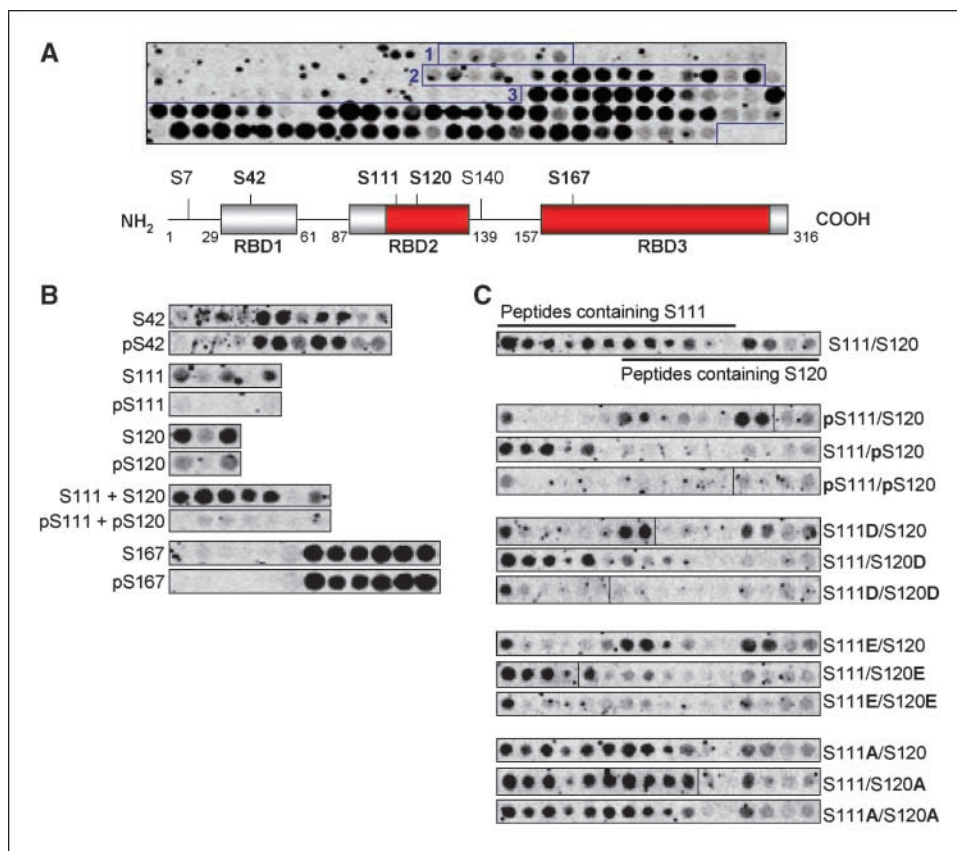


**Figure 3.** Sprouty2 phosphorylation within RBD2 inhibits B-Raf binding. *A, top*, binding of [<sup>35</sup>S]methionine-labeled *in vitro* transcribed and translated HA-tagged B-Raf to a Sprouty2 peptide array, composed of 23-mer peptides each shifted by two residues. RBD1-3 were detected (boxed peptide spots). *Bottom*, schematic representation of mouse Sprouty2 protein indicating RBD1-3 (gray boxes) positions. *Red*, higher-affinity B-Raf binding. Sprouty2 phosphorylation sites within these domains are in bold. *B*, [<sup>35</sup>S]methionine-labeled HA-tagged B-Raf binding to arrayed Sprouty2 peptides with serine or phosphoserine residues. *C*, [<sup>35</sup>S]methionine-labeled HA-tagged B-Raf binding to arrayed Sprouty2 peptides with aspartate, glutamate, or alanine substitutions at Ser<sup>111</sup> and/or Ser<sup>120</sup>.

## Results

**Sprouty2 phosphorylation regulates the association with B-Raf.** When WCL from HEK293 cells transfected with FLAG-tagged Sprouty2 and either wild-type or an activated oncogenic form of myc-tagged B-Raf (V600E) were run on SDS-PAGE beside anti-Myc immunoprecipitations, only the fastest-migrating Sprouty2 electrophoretic variant copurified with wild-type B-Raf (Fig. 1A). Although the distribution of Sprouty2 electrophoretic forms was relatively equal when cotransfected with wild-type B-Raf, there was a shift toward the slower forms in cells expressing B-Raf V600E, with markedly less of the fastest-migrating form that had associated with wild-type B-Raf (Fig. 1A). The shift from fast to slow electrophoretic variants was observed when Sprouty2 was cotransfected with B-Raf V600E or constitutively active MEK1 (MEK:EE; ref. 33), accompanied by increased ERK1 and ERK2 phosphorylation (pERK1/2), suggesting that the mobility shift resulted from MAPK activation (Fig. 1B). It should be noted that typically only two electrophoretic forms are consistently well-separated on SDS-PAGE (e.g., Fig. 1B); separation into three forms is variable likely due to variations in electrophoresis conditions. Consistent with previous results (34), the slower-migrating Sprouty2 could be shifted to the faster form when immunoprecipitated protein was incubated with calf intestinal phosphatase (Fig. 1C, left). Furthermore, in cells metabolically labeled with [<sup>32</sup>P]orthophosphate, coexpression of B-Raf V600E resulted in increased Sprouty2 phosphorylation (Fig. 1C, right, top). The <sup>32</sup>P-labeled Sprouty2 band comigrated with the slower-migrating Coomassie-stained band, consistent with the mobility shift resulting from phosphorylation (Fig. 1C, right, bottom). These results indicate that B-Raf preferentially associates with faster

mobility hypophosphorylated Sprouty2 and suggest that MAPK activation leads to Sprouty2 phosphorylation and reduced B-Raf association. In support of this conclusion, we determined using quantitative direct scanning of Western blots and near-infrared fluorophore-conjugated secondary antibodies that binding of recombinant GST-B-Raf catalytic domain was reduced by 40% if immunoprecipitated Sprouty2 had been coexpressed with active MEK:EE, which was reversed by phosphatase pretreatment of the immunoprecipitated Sprouty2 (Fig. 1D). The reduced B-Raf binding was associated with a MEK1-induced Sprouty2 mobility shift, which also was reversed by phosphatase (Fig. 1D), consistent with Sprouty2 phosphorylation negatively regulating B-Raf binding. Interestingly, B-Raf association was higher (150%) and the proportion of fast-migrating Sprouty2 was greater following phosphatase treatment than for Sprouty2 immunoprecipitated from cells not expressing MEK:EE, suggesting that basal Sprouty2 phosphorylation influenced B-Raf binding and electrophoretic mobility (Fig. 1D). As a result, there was >2-fold difference in B-Raf binding of Sprouty2 coexpressed with active MEK without or with phosphatase treatment, indicating the contribution of phosphorylation in modifying this interaction. These results indicate that MAPK activation by oncogenic B-Raf results in a higher proportion and/or stoichiometry of Sprouty2 phosphorylation that antagonizes B-Raf binding.

**Sprouty2 is phosphorylated on multiple serine residues.** To identify B-Raf-induced Sprouty2 phosphorylation sites, we purified Sprouty2 expressed with or without B-Raf V600E and analyzed tryptic fragments by mass spectrometry using a precursor ion scan of *m/z* -79 on a triple-quadrupole instrument in negative ion mode followed by an ion-trap high-resolution scan, which produces a mass spectrum that contains only the molecular ions of the

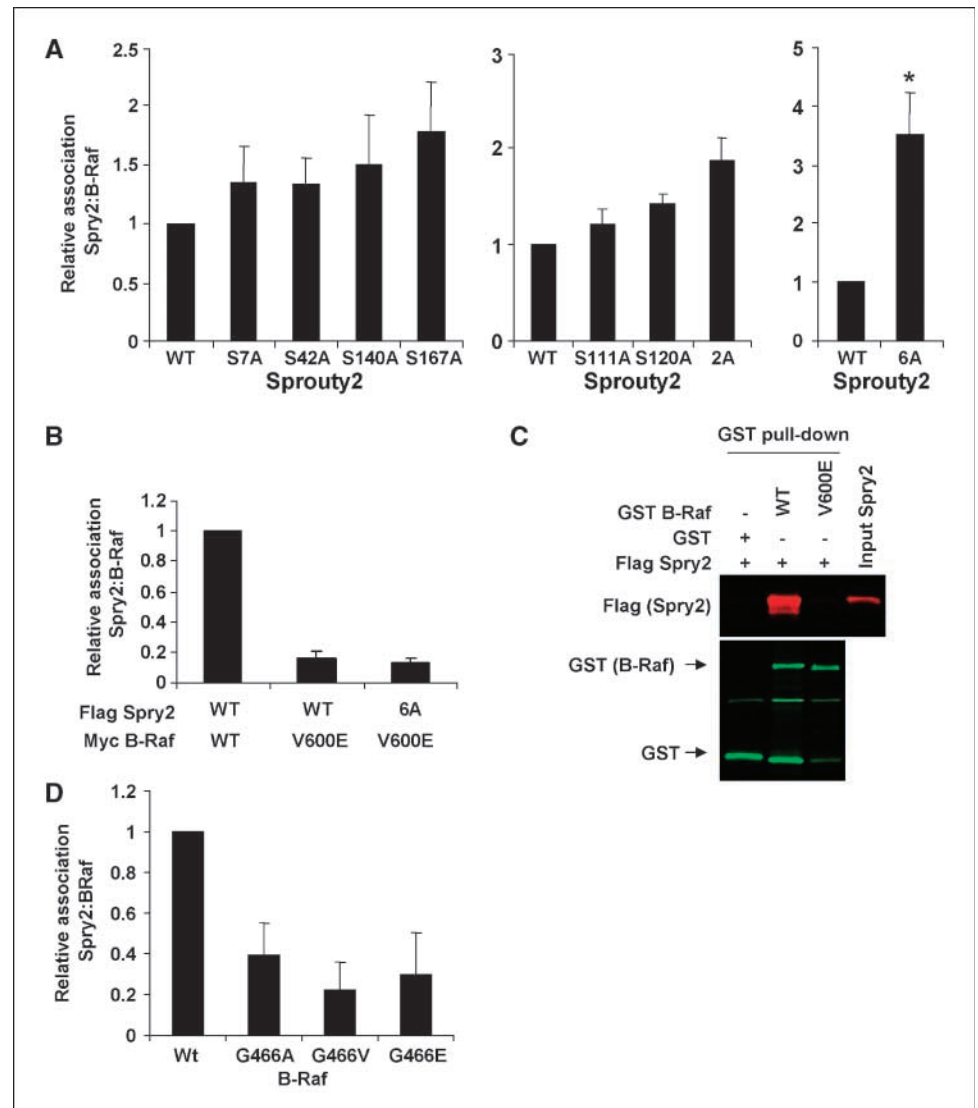
phosphopeptides present in the sample (32). Although no basal Sprouty2 phosphorylation was detected (Fig. 2A, left), four sites were identified (Ser<sup>7</sup>, Ser<sup>42</sup>, Ser<sup>140</sup>, and Ser<sup>167</sup>; numbering = mouse Sprouty2) when coexpressed with B-Raf V600E (Fig. 2A, right). All lie within the Sprouty2 NH<sub>2</sub>-terminal half and are highly conserved in vertebrate species (Fig. 2A, bottom).

Individual mutations to nonphosphorylatable alanines (S7A, S42A, S140A, and S167A) did not significantly affect the B-Raf V600E-induced Sprouty2 mobility shift (Fig. 2B). It was reported previously that epidermal growth factor-induced phosphorylation of two sites on human Sprouty2 corresponding to Ser<sup>111</sup> and Ser<sup>120</sup> resulted in slower Sprouty2 electrophoretic mobility (35). We found that mutation of either site to alanine (S111A and S120A) reduced but did not completely reverse the B-Raf V600E-induced mobility shift (Fig. 2B), suggesting that these sites were also modified downstream of B-Raf. Mutation of the four phosphorylation sites identified by mass spectrometry (4A) did not affect Sprouty2 mobility (Fig. 2C) but did result in a loss in Sprouty2 phosphorylation detectable by mass spectrometry (Supplementary Fig. S1B). Mutation of both S111 and S120 to alanines (2A) completely abolished the B-Raf

V600E-induced mobility shift (Fig. 2C). Furthermore, <sup>32</sup>P incorporation on *Escherichia coli*-expressed GST-Sprouty2 induced by incubation with WCL from B-Raf V600E-expressing HEK293 cells was markedly diminished in the 6A mutant compared with wild-type Sprouty2 (Fig. 2D). Based on the direct and indirect evidence (identification by mass spectrometry, electrophoretic mobility shift, and <sup>32</sup>P incorporation), we have identified six serine residues that appear to be the principal phosphorylation sites modified in response to MAPK activation, with the caveat that there may be additional minor phosphorylation sites not detected by mass spectrometry or that may not influence Sprouty2 electrophoretic mobility.

**Sprouty2 phosphorylations cooperate to regulate B-Raf binding.** Having identified B-Raf-induced Sprouty2 phosphorylations, we next determined where B-Raf bound to Sprouty2 and whether specific phosphorylations affected B-Raf binding. A peptide array consisting of 23-mers, each consecutively shifted by two residues and spanning the entire Sprouty2 protein, was incubated with [<sup>35</sup>S]methionine-labeled wild-type B-Raf produced *in vitro* transcription and translation. The pattern of <sup>35</sup>S labeling revealed direct interactions between B-Raf and three distinct

**Figure 4.** Effect of mutating Sprouty2 phosphorylation sites on binding to wild-type or cancer-associated B-Raf mutants. **A**, FLAG-Sprouty2 wild-type or phosphorylation site mutants were transfected with Myc-B-Raf V600E. Myc immunoprecipitates and WCL were Western blotted for FLAG or Myc. Sprouty2 association with B-Raf expressed relative to total Sprouty2. Mean  $\pm$  SE, normalized to Sprouty2 wild-type binding to B-Raf. Left,  $n = 7$ ; middle,  $n = 3$ ; right,  $n = 3$ . \*,  $P < 0.05$ , significant difference from wild-type Sprouty2 binding (Student's *t* test). **B**, FLAG-Sprouty2 wild-type or phosphorylation site mutants were transfected with Myc wild-type B-Raf or Myc-B-Raf V600E. Myc immunoprecipitates and WCL were Western blotted for FLAG or Myc. Mean  $\pm$  SE ( $n = 12$ ), normalized to binding of Sprouty2 wild-type to B-Raf wild-type. **C**, GST, GST-B-Raf wild-type, or GST-B-Raf V600E were incubated with recombinant FLAG-Sprouty2, recovered on glutathione Sepharose beads (GST pull-down), and analyzed for B-Raf and associated Sprouty2 by Western blotting for GST and FLAG. Input FLAG-Sprouty2 was loaded as a positive control. **D**, FLAG-Sprouty2 was transiently transfected with cancer-associated Myc-B-Raf G466 P-loop mutants. Myc immunoprecipitates and WCL were Western blotted for FLAG or Myc. Mean  $\pm$  SE ( $n = 4$ ), normalized to Sprouty2 binding to wild-type B-Raf.



Sprouty2 regions that we named Raf binding domains (RBD) 1-3 (Fig. 3A). Interaction with RBD1 was relatively weak, whereas regions of strong binding were detected within RBD2 and RBD3 (Fig. 3A, red). Four of the six Sprouty2 phosphorylation sites modified in the presence of B-Raf (S42, S111, S120, and S167) lie within these binding domains (Fig. 3A). B-Raf binding to peptides with corresponding phosphoserine residues was reduced for pS111 and pS120 but not for pS42 or pS167 (Fig. 3B). Given that in the initial phosphopeptide array many peptides containing pS111 also contained pS120, we examined whether phosphorylation of either site individually would inhibit B-Raf binding. Individual substitution of either S111 or S120 with phosphoserine inhibited B-Raf binding and no binding was observed when both sites were substituted

(Fig. 3C). Similarly, phosphomimetic aspartate or glutamate substitutions at either site inhibited B-Raf binding. Finally, substitution of S111 or S120 with alanine had no effect on B-Raf association, indicating that alanines were equivalent to nonphosphorylated serines (Fig. 3C; summarized in Supplementary Table S1). Collectively, these results indicate that B-Raf directly binds Sprouty2 at three domains and that phosphorylation of Ser<sup>111</sup> or Ser<sup>120</sup> within RBD2 inhibits this interaction. A similar pattern of phosphorylation-regulated interaction was observed with Raf-1, indicating that it is likely a general phenomenon for Raf kinases (data not shown).

We next investigated how Sprouty2 phosphorylation affected B-Raf binding in cells. Individual mutation of S7, S42, S140, or S167 to alanines had no effect on Sprouty2 binding to wild-type

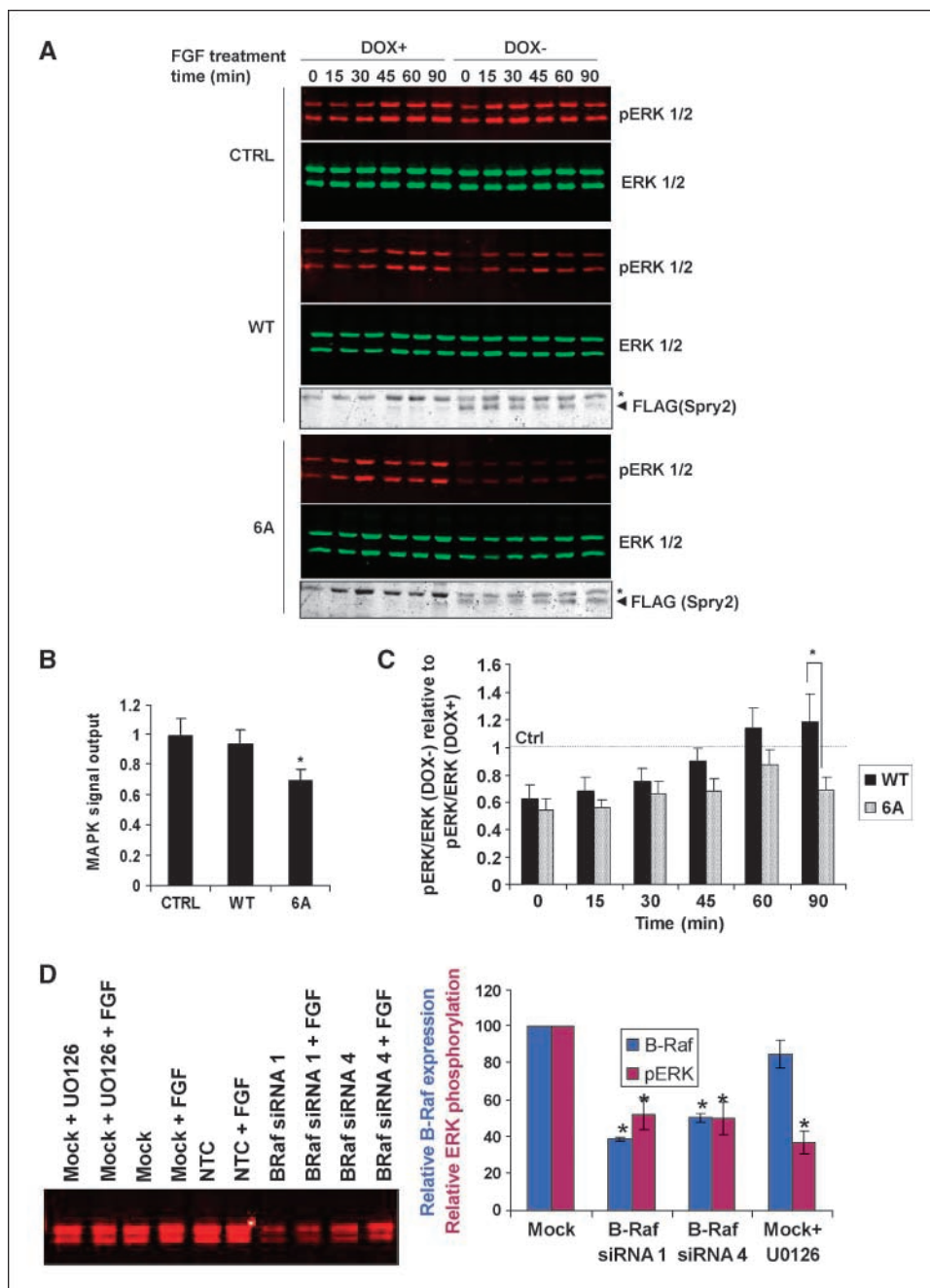


**Figure 5.** Inhibition of FGF-stimulated ERK activation by Sprouty2 phosphorylation site mutant. **A**, NIH3T3 Tet-Off FLAG-Sprouty2 control (CTRL), wild-type (WT; clone 2 shown), or 6A (clone 3 shown) cell lines were cultured with or without doxycycline, stimulated with FGF for the times indicated, and Western blotted for pERK, ERK, and FLAG-Sprouty2. Arrowhead, FLAG-Sprouty2. **B**, FGF-induced MAPK signal output following Sprouty2 induction relative to uninduced condition was determined from areas under the curve of time-course experiments. pERK/ERK for DOX- (Sprouty2-induced) conditions expressed relative to pERK/ERK for DOX+ (uninduced) conditions were plotted for each time point and areas under the curve were calculated using the trapezoidal rule. Mean  $\pm$  SE, normalized to control clone, from four (control) or seven (wild-type and 6A) repetitions. \*,  $P < 0.05$ , significant difference from wild-type (Student's  $t$  test). **C**, ratios of pERK/ERK for DOX- (Sprouty2-induced) conditions expressed relative to pERK/ERK for DOX+ (uninduced) for each time point for wild-type or 6A Sprouty2. Mean  $\pm$  SE ( $n = 7$ ), normalized to control clone. \*,  $P < 0.05$ , significant difference between wild-type and 6A (Student's  $t$  test). **D**, NIH3T3 cells were mock transfected or transfected with nontargeting control (NTC) or B-Raf siRNAs. After 48 h, cells were treated with FGF as above for 45 min either with or without 10  $\mu$ Mol/L U0126. B-Raf expression levels were determined by quantitative Western blotting (left), and the relative expression of B-Raf (right, dark blue) and the ratio of pERK/ERK (right, burgundy) were determined for these conditions. Mean  $\pm$  SE ( $n = 6$ ), normalized to mock transfectant. \*,  $P < 0.01$ , significant difference from mock transfectant (Student's  $t$  test).

B-Raf (Fig. 4A, left; Supplementary Fig. S2A). Although individual mutation to S111A or S120A had no significant effect on B-Raf binding, mutation of both increased binding almost 2-fold (Fig. 4A, middle; Supplementary Fig. S2B). Intriguingly, when all six sites were mutated to alanines there was a significant ~3.5-fold increase in B-Raf binding (Fig. 4A, right; Supplementary Fig. S2C). Therefore, although mutation of S7, S42, S140, or S167 individually had little effect on B-Raf association, collective phosphorylation of these sites likely cooperates with S111 and S120 phosphorylation within RBD2 to inhibit B-Raf binding.

**Oncogenic B-Raf mutants do not bind Sprouty2 independent of phosphorylation status.** We found previously that Sprouty2 did not bind to B-Raf V600E (11) and postulated that this could be due to B-Raf-induced Sprouty2 phosphorylation (Fig. 1A). Because the Sprouty2 6A mutant displayed enhanced binding to wild-type B-Raf (Fig. 4A; Supplementary Fig. S2C), we examined whether inhibiting phosphorylation on these sites would restore B-Raf V600E binding. Surprisingly, Sprouty2 association with B-Raf V600E was unaffected by the 6A mutations (Fig. 4B; Supplementary Fig. S3A). Similarly, although recombinant nonphosphorylated FLAG-Sprouty2 associated with recombinant GST-B-Raf wild-type catalytic domain *in vitro*, it did not associate with the V600E mutant (Fig. 4C). These results indicate that although Sprouty2 phosphorylation inhibits wild-type B-Raf binding, the V600E B-Raf mutant resists Sprouty2 binding independent of phosphorylation status. One possible explanation is that B-Raf mutations that induce active kinase conformations prevent Sprouty2 binding. We therefore tested three B-Raf mutants that lie within the glycine-rich P-loop that either modestly increase (G466A) or impair (G466E and G466V) kinase activity but induce an active kinase conformation in each case (36). Similar to B-Raf V600E, they did not significantly bind Sprouty2 relative to wild-type B-Raf (Fig. 4D; Supplementary Fig. S3B), consistent with our previous observation that the oncogenic activation loop B-Raf mutants L597V, V600D, and K601E did not bind Sprouty2 (11). These results indicate that there are two independent factors influencing the B-Raf/Sprouty2 interaction: Sprouty2 phosphorylation and B-Raf kinase domain conformation.

**Sprouty2 phosphorylation influences MAPK activation.** Given that Sprouty2 phosphorylation affects wild-type B-Raf binding, we tested whether the 6A mutant would have an enhanced ability to repress MAPK activation by FGF. We generated NIH3T3 cells expressing tetracycline-regulated (Tet-Off) wild-type or 6A mutant Sprouty2. Three wild-type and three 6A Sprouty2 cell lines were selected for their relatively comparable Sprouty2 expression following doxycycline withdrawal (Supplementary Fig. S4). A control nonexpressing clone was also established using the empty tetracycline-responsive vector. FGF treatment of the control cells resulted in increased phosphorylated ERK1 and ERK2 that were sustained over 90 min, which was unaffected by doxycycline withdrawal (Fig. 5A, top). In contrast, ERK activation was somewhat inhibited when wild-type Sprouty2 was induced following doxycycline removal, consistent with Sprouty2 being an inhibitor of FGF-induced MAPK activation (ref. 37; Fig. 5A, middle). Inhibition of ERK activation was more pronounced in 6A Sprouty2-expressing cells relative to wild-type Sprouty2 (Fig. 5A, bottom). When the areas under the curve for active ERK levels over time were calculated as a measure of signal output (38), 6A Sprouty2 induction significantly inhibited MAPK signal output relative to wild-type Sprouty2 (Fig. 5B). Although ERK activation in 6A Sprouty2-expressing cells was lower at every time point, the differences between wild-type and 6A Sprouty2 did not achieve statistical significance until 90 min

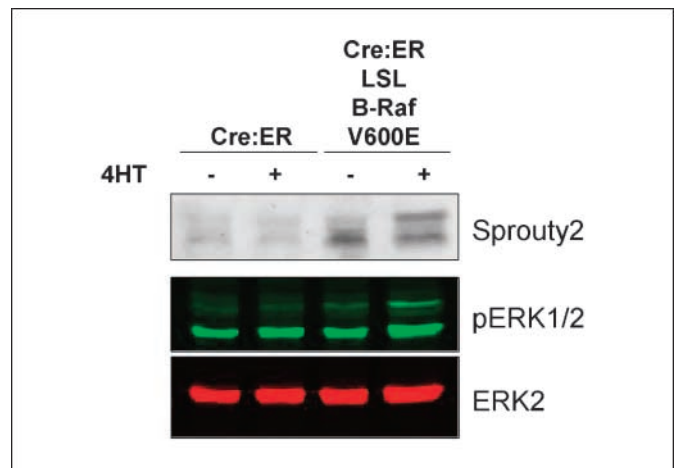


**Figure 6.** Mobility shift of endogenous Sprouty2 induced by endogenous V600E B-Raf. Mouse embryo fibroblasts expressing conditionally active Cre:ER alone or in combination with a heterozygous knock-in V600E B-Raf mutation preceded by a Lox-Stop-Lox (LSL) cassette were either left untreated or treated with 50 nmol/L 4-hydroxytamoxifen (4HT) for 96 h to induce Cre-mediated recombination. Sprouty2, pERK1/2, and ERK2 levels were determined by quantitative Western blotting.

(Fig. 5C). One interpretation is that wild-type Sprouty2 inhibits FGF-induced MAPK activation, with Sprouty2 phosphorylation at later time points reducing this inhibitory effect. In contrast, the 6A Sprouty2 mutant is not phosphorylated on critical sites and MAPK inhibition persists, decreasing MAPK signal output. Therefore, Sprouty2 phosphorylation may act as an additional regulatory mechanism to control MAPK signaling. Consistent with Sprouty2 inhibition of B-Raf being the cause of reduced MAPK activation, B-Raf knockdown with two independent siRNA duplexes (Fig. 5D, left) resulted in proportionate and significant reduction in MAPK activation (Fig. 5D, right).

**Endogenous Sprouty2 phosphorylation downstream of endogenous V600E B-Raf.** We examined how endogenous oncogenic V600E B-Raf affected the mobility of endogenous Sprouty2 in mouse embryonic fibroblasts (30). Mouse embryonic fibroblasts from mice that expressed a conditionally activated Cre-strogen receptor (Cre:ER) alone or in combination with a heterozygous knock-in V600E B-Raf mutation preceded by a Lox-Stop-Lox cassette (39) were either left untreated or treated with 50 nmol/L 4-hydroxytamoxifen for 96 h to induce Cre-mediated recombination (Fig. 6). Sprouty2 levels were low in Cre:ER-expressing mouse embryonic fibroblasts either with or without 4-hydroxytamoxifen. In the absence of 4-hydroxytamoxifen, Sprouty2 levels were higher in Cre:ER; Lox-Stop-Lox B-Raf V600E mouse embryonic fibroblasts likely due to inherent leakiness of the Cre:ER transgene; however, following 4-hydroxytamoxifen treatment, Sprouty2 levels were further increased with a significant proportion shifted to the slower mobility form. Although 4-hydroxytamoxifen did not increase pERK1/2 levels in Cre:ER-expressing mouse embryonic fibroblasts, there was an ~1.8-fold increase in total pERK1/2 staining Cre:ER; Lox-Stop-Lox B-Raf V600E mouse embryonic fibroblasts following 4-hydroxytamoxifen treatment. These data indicate that endogenous V600E B-Raf is sufficient to induce phosphorylation of endogenous Sprouty2.

## Discussion

Sprouty regulation of receptor tyrosine kinase signaling is complex, because it acts at multiple levels and may have apparently

positive and negative actions within the same pathway. That being said, one way Sprouty proteins regulate MAPK signaling is through direct association with Raf kinases (11, 25–28). We observed that B-Raf binding is negatively regulated by Sprouty2 phosphorylation on six serine residues that act in concert; two sites (Ser<sup>111</sup> and Ser<sup>120</sup>) directly affect binding, whereas the remaining four appear to contribute indirectly, possibly by affecting protein conformation. Furthermore, Sprouty2 was unable to associate with B-Raf mutants that adopt active kinase conformations. Therefore, we propose that there are two independent factors that affect the Sprouty/B-Raf interaction: Sprouty2 phosphorylation and B-Raf kinase conformation. These findings have important implications for MAPK signaling in normal and cancer cells.

A significant observation from this study is that activated B-Raf mutants do not bind Sprouty2 regardless of its phosphorylation status. These findings are consistent with, and provide some mechanistic detail for, a recent publication reporting that B-Raf V600E evades a feedback inhibition response that includes elevated Sprouty2 (21).

Sprouty gene transcription is regulated by the MAPK pathway (40, 41), consistent with their role as negative feedback regulators, and oncogenic mutations in melanoma and gastrointestinal stromal tumors that activate MAPK also lead to elevated Sprouty levels (11, 20–23). At the same time, Sprouty2 phosphorylation is increased in response to MAPK activation, thereby reducing the ability of Sprouty2 to bind B-Raf and to inhibit FGF activation of MAPK (Figs. 4 and 5). Therefore, it appears that the MAPK pathway both transcriptionally up-regulates Sprouty2 and posttranscriptionally attenuates its ability to inhibit MAPK signaling. One possible reason for this arrangement is that Sprouty may be regulated via transcription at a gross level in response to chronic MAPK activation, but once protein levels have been elevated, a further level of acute control may be exerted by varying the phosphorylation-dephosphorylation status. This possibility suggests that Sprouty

proteins may not act as simple on/off switches but might be tunable regulators that influence MAPK signaling kinetics, duration, magnitude, and signal output. If phosphorylation inhibits the ability of Sprouty2 to repress B-Raf, then it would be predicted that dephosphorylation should increase Sprouty2-mediated MAPK inhibition. Consistent with this possibility, we found that the 6A mutant was significantly better at suppressing FGF-induced MAPK activation at later time points (Fig. 5), whereas it was recently reported that *Xenopus laevis* Sprouty2 does not influence acute ERK activation by FGF but does regulate the duration of ERK activity (42).

In conclusion, we have established that the ability of Sprouty2 to act as an inhibitor of B-Raf activity and the MAPK pathway is under dual control by two independent mechanisms: posttranslational phosphorylation of Sprouty2 and B-Raf kinase conformation. The phosphorylation status of specific residues on Sprouty2 influences its ability to interact with B-Raf and to modulate MAPK activation in response to growth factors, whereas evidence suggests that the active B-Raf kinase conformation independently prevents association with Sprouty2. Delineation of the precise signaling pathway leading to Sprouty phosphorylation is an important future goal in light of the important implications these findings have for MAPK signaling in normal and cancer cells.

## Disclosure of Potential Conflicts of Interest

No potential conflicts of interest were disclosed.

## Acknowledgments

Received 11/21/08; revised 5/27/09; accepted 6/25/09; published OnlineFirst 8/18/09.

**Grant support:** Cancer Research UK and NIH grant CA030721 (M.F. Olson) and Medical Research Council and RASOR IRColl grant for Proteomic Technology funded by the BBSRC and EPSRC (N.A. Morrice).

The costs of publication of this article were defrayed in part by the payment of page charges. This article must therefore be hereby marked *advertisement* in accordance with 18 U.S.C. Section 1734 solely to indicate this fact.

## References

- Hacohen N, Kramer S, Sutherland D, Hiromi Y, Krasnow MA. Sprouty encodes a novel antagonist of FGF signaling that patterns apical branching of the *Drosophila* airways. *Cell* 1998;92:253–63.
- de Maximy AA, Nakatake Y, Moncada S, Itoh N, Thiery JP, Bellusci S. Cloning and expression pattern of a mouse homologue of *Drosophila* sprouty in the mouse embryo. *Mech Dev* 1999;81:213–6.
- Tefft JD, Lee M, Smith S, et al. Conserved function of mSpry-2, a murine homologue of *Drosophila* sprouty, which negatively modulates respiratory organogenesis. *Curr Biol* 1999;9:219–22.
- Minowada G, Jarvis LA, Chi CL, et al. Vertebrate Sprouty genes are induced by FGF signaling and can cause chondrodysplasia when overexpressed. *Development* 1999;126:4465–75.
- Kim HJ, Bar-Sagi D. Modulation of signalling by Sprouty: a developing story. *Nat Rev Mol Cell Biol* 2004;5:441–50.
- Mason JM, Morrison DJ, Basson MA, Licht JD. Sprouty proteins: multifaceted negative-feedback regulators of receptor tyrosine kinase signaling. *Trends Cell Biol* 2006; 16:45–54.
- Ishida M, Ichihara M, Mii S, et al. Sprouty2 regulates growth and differentiation of human neuroblastoma cells through RET tyrosine kinase. *Cancer Sci* 2007;98: 815–21.
- Lee CC, Putnam AJ, Miranti CK, et al. Overexpression of sprouty 2 inhibits HGF/SF-mediated cell growth, invasion, migration, and cytokinesis. *Oncogene* 2004;23: 5193–202.
- Edwin F, Singh R, Endersby R, Baker SJ, Patel TB. The tumor suppressor PTEN is necessary for human Sprouty 2-mediated inhibition of cell proliferation. *J Biol Chem* 2006;281:4816–22.
- Minowada G, Miller YE. Overexpression of Sprouty 2 in mouse lung epithelium inhibits urethane-induced tumorigenesis. *Am J Respir Cell Mol Biol* 2009;40:31–7.
- Tsavachidou D, Coleman ML, Athanasiadis G, et al. SPRY2 is an inhibitor of the ras/extracellular signal-regulated kinase pathway in melanocytes and melanoma cells with wild-type BRAF but not with the V599E mutant. *Cancer Res* 2004;64:5556–9.
- Shaw AT, Meissner A, Dowdle JA, et al. Sprouty-2 regulates oncogenic K-ras in lung development and tumorigenesis. *Genes Dev* 2007;21:694–707.
- Lee SA, Ho C, Roy R, et al. Integration of genomic analysis and *in vivo* transfection to identify sprouty 2 as a candidate tumor suppressor in liver cancer. *Hepatology* 2008;47:1200–10.
- Fong CW, Chua MS, McKie AB, et al. Sprouty 2, an inhibitor of mitogen-activated protein kinase signaling, is down-regulated in hepatocellular carcinoma. *Cancer Res* 2006;66:2048–58.
- Sutterluty H, Mayer CE, Setinek U, et al. Down-regulation of Sprouty2 in non-small cell lung cancer contributes to tumor malignancy via extracellular signal-regulated kinase pathway-dependent and -independent mechanisms. *Mol Cancer Res* 2007;5:509–20.
- Fritzschke S, Kenzelmann M, Hoffmann MJ, et al. Concomitant down-regulation of SPRY1 and SPRY2 in prostate carcinoma. *Endocr Relat Cancer* 2006; 13:839–49.
- Wang J, Thompson B, Ren C, Ittmann M, Kwabi-Addo B. Sprouty4, a suppressor of tumor cell motility, is down regulated by DNA methylation in human prostate cancer. *Prostate* 2006;66:613–24.
- McKie AB, Douglas DA, Olijslagers S, et al. Epigenetic inactivation of the human Sprouty2 (hSPRY2) homologue in prostate cancer. *Oncogene* 2005;24:2166–74.
- Lo TL, Fong CW, Yusoff P, et al. Sprouty and cancer: the first terms report. *Cancer Lett* 2006;242:141–50.
- Bloethner S, Chen B, Hemminki K, et al. Effect of common B-RAF and N-RAS mutations on global gene expression in melanoma cell lines. *Carcinogenesis* 2005; 26:1224–32.
- Pratilas CA, Taylor BS, Ye Q, et al. V600EBRAF is associated with disabled feedback inhibition of RAF-MEK signaling and elevated transcriptional output of the pathway. *Proc Natl Acad Sci U S A* 2009;106:4519–24.
- Nielsen TO, West RB, Linn SC, et al. Molecular characterisation of soft tissue tumours: a gene expression study. *Lancet* 2002;359:1301–7.
- Frolov A, Chahwan S, Ochs M, et al. Response markers and the molecular mechanisms of action of Gleevec in gastrointestinal stromal tumors. *Mol Cancer Ther* 2003;2:699–709.
- Cabrita MA, Christofori G. Sprouty proteins, masterminds of receptor tyrosine kinase signaling. *Angiogenesis* 2008;11:53–62.
- Reich A, Sapir A, Shilo B. Sprouty is a general inhibitor of receptor tyrosine kinase signaling. *Development* 1999;126:4139–47.



26. Sasaki A, Taketomi T, Kato R, et al. Mammalian Sprouty4 suppresses Ras-independent ERK activation by binding to Raf1. *Nat Cell Biol* 2003;5:427–32.
27. Yusoff P, Lao DH, Ong SH, et al. Sprouty2 inhibits the Ras/MAP kinase pathway by inhibiting the activation of Raf. *J Biol Chem* 2002;277:3195–201.
28. Aranda S, Alvarez M, Turro S, Laguna A, de la Luna S. Sprouty2-mediated inhibition of fibroblast growth factor signaling is modulated by the protein kinase DYRK1A. *Mol Cell Biol* 2008;28:5899–911.
29. Sahai E, Olson MF. Purification of TAT-C3 exoenzyme. *Methods Enzymol* 2006;406:128–40.
30. Mercer K, Giblett S, Green S, et al. Expression of endogenous oncogenic V600E-raf induces proliferation and developmental defects in mice and transformation of primary fibroblasts. *Cancer Res* 2005;65:11493–500.
31. Campbell D, Morrice N. Identification of protein phosphorylation sites by a combination of mass spectrometry and solid phase Edman sequencing. *J Biomol Tech* 2002;13:119–30.
32. Williamson BL, Marchese J, Morrice NA. Automated identification and quantification of protein phosphorylation sites by LC/MS on a hybrid triple quadrupole linear ion trap mass spectrometer. *Mol Cell Proteomics* 2006;5:337–46.
33. Alessi DR, Saito Y, Campbell DG, et al. Identification of the sites in MAP kinase kinase-1 phosphorylated by p74raf-1. *EMBO J* 1994;13:1610–9.
34. Impagnatiello MA, Weitzer S, Gannon G, Compagni A, Cotten M, Christofori G. Mammalian sprouty-1 and -2 are membrane-anchored phosphoprotein inhibitors of growth factor signaling in endothelial cells. *J Cell Biol* 2001;152:1087–98.
35. DaSilva J, Xu L, Kim HJ, Miller WT, Bar-Sagi D. Regulation of sprouty stability by Mnk1-dependent phosphorylation. *Mol Cell Biol* 2006;26:1898–907.
36. Wan PT, Garnett MJ, Roe SM, et al. Mechanism of activation of the RAF-ERK signaling pathway by oncogenic mutations of B-RAF. *Cell* 2004;116:855–67.
37. Hanafusa H, Torii S, Yasunaga T, Nishida E. Sprouty1 and Sprouty2 provide a control mechanism for the Ras/MAPK signalling pathway. *Nat Cell Biol* 2002;4:850–8.
38. Mayawala K, Gelmi CA, Edwards JS. MAPK cascade possesses decoupled controllability of signal amplification and duration. *Biophys J* 2004;87:L01–2.
39. Wickenden JA, Jin H, Johnson M, et al. Colorectal cancer cells with the BRAF(V600E) mutation are addicted to the ERK1/2 pathway for growth factor-independent survival and repression of BIM. *Oncogene* 2008;27:7150–61.
40. Ozaki K, Kadamoto R, Asato K, Tanimura S, Itoh N, Kohno M. ERK pathway positively regulates the expression of Sprouty genes. *Biochem Biophys Res Commun* 2001;285:1084–8.
41. Sasaki A, Taketomi T, Wakioka T, Kato R, Yoshimura A. Identification of a dominant negative mutant of Sprouty that potentiates fibroblast growth factor- but not epidermal growth factor-induced ERK activation. *J Biol Chem* 2001;276:36804–8.
42. Hanafusa H, Matsumoto K, Nishida E. Regulation of ERK activity duration by Sprouty contributes to dorsoventral patterning. *Nat Cell Biol* 2009;11:106–9.

# Cancer Research

The Journal of Cancer Research (1916–1930) | The American Journal of Cancer (1931–1940)

## Sprouty2 Association with B-Raf Is Regulated by Phosphorylation and Kinase Conformation

Suzanne C. Brady, Mathew L. Coleman, June Munro, et al.

*Cancer Res* 2009;69:6773-6781. Published OnlineFirst August 18, 2009.

<b>Updated version</b>	Access the most recent version of this article at: doi: <a href="https://doi.org/10.1158/0008-5472.CAN-08-4447">10.1158/0008-5472.CAN-08-4447</a>
<b>Supplementary Material</b>	Access the most recent supplemental material at: <a href="http://cancerres.aacrjournals.org/content/suppl/2009/08/03/0008-5472.CAN-08-4447.DC1">http://cancerres.aacrjournals.org/content/suppl/2009/08/03/0008-5472.CAN-08-4447.DC1</a>

<b>Cited articles</b>	This article cites 42 articles, 17 of which you can access for free at: <a href="http://cancerres.aacrjournals.org/content/69/17/6773.full#ref-list-1">http://cancerres.aacrjournals.org/content/69/17/6773.full#ref-list-1</a>
<b>Citing articles</b>	This article has been cited by 10 HighWire-hosted articles. Access the articles at: <a href="http://cancerres.aacrjournals.org/content/69/17/6773.full#related-urls">http://cancerres.aacrjournals.org/content/69/17/6773.full#related-urls</a>

<b>E-mail alerts</b>	<a href="#">Sign up to receive free email-alerts</a> related to this article or journal.
<b>Reprints and Subscriptions</b>	To order reprints of this article or to subscribe to the journal, contact the AACR Publications Department at <a href="mailto:pubs@aacr.org">pubs@aacr.org</a> .
<b>Permissions</b>	To request permission to re-use all or part of this article, use this link <a href="http://cancerres.aacrjournals.org/content/69/17/6773">http://cancerres.aacrjournals.org/content/69/17/6773</a> . Click on "Request Permissions" which will take you to the Copyright Clearance Center's (CCC) Rightslink site.